Evolutionary Advantage Conferred by an Eukaryote-to-Eukaryote Gene Transfer Event in Wine Yeasts

Souhir Marsit,[1,2,3] Adriana Mena,[4] Frédéric Bigey,[1,2,3] François-Xavier Sauvage,[1,2,3] Arnaud Couloux,[5] Julie Guy,[5] Jean-Luc Legras,[1,2,3] Eladio Barrio,[4] Sylvie Dequin,[1,2,3] and Virginie Galeote*[,1,2,3]

[1]INRA, UMR1083, SPO, F-34060 Montpellier, France

[2]Montpellier SupAgro, UMR1083, SPO, F-34060 Montpellier, France

[3]Montpellier University, UMR1083, SPO, F-34060 Montpellier, France

[4]Department of Genetics, University of Valencia, and Department of Biotechnology, Institute of Agrochemistry and Food Technology, CSIC, Valencia, Spain

[5]CEA, Institut de Génomique, Genoscope, Centre National de Séquençage, Evry, France

***Corresponding author:** E-mail: galeote@supagro.inra.fr.

Associate editor: Csaba Pal

Abstract

Although an increasing number of horizontal gene transfers have been reported in eukaryotes, experimental evidence for their adaptive value is lacking. Here, we report the recent transfer of a 158-kb genomic region between *Torulaspora microellipsoides* and *Saccharomyces cerevisiae* wine yeasts or closely related strains. This genomic region has undergone several rearrangements in *S. cerevisiae* strains, including gene loss and gene conversion between two tandemly duplicated *FOT* genes encoding oligopeptide transporters. We show that *FOT* genes confer a strong competitive advantage during grape must fermentation by increasing the number and diversity of oligopeptides that yeast can utilize as a source of nitrogen, thereby improving biomass formation, fermentation efficiency, and cell viability. Thus, the acquisition of *FOT* genes has favored yeast adaptation to the nitrogen-limited wine fermentation environment. This finding indicates that anthropic environments offer substantial ecological opportunity for evolutionary diversification through gene exchange between distant yeast species.

Key words: **HGT, domestication, competition, nitrogen, oligopeptides, *FOT* genes.**

Introduction

Horizontal gene transfer (HGT), the acquisition of new genes from distantly related species, has been established as a dominant force for prokaryotic evolution (Koonin and Wolf 2008) and is increasingly recognized as a prominent source of adaptation in eukaryotes. With the availability of sequence data for numerous eukaryotic genomes, many examples of HGT from prokaryotes to eukaryotes and, increasingly, from eukaryotes to eukaryotes have been reported, in particular among fungi (Keeling and Palmer 2008; Andersson 2009; Marcet-Houben and Gabaldon 2009; Gladieux et al. 2014).

HGT is a means by which organisms can rapidly acquire new biological functions (Keeling and Palmer 2008), facilitating their specialization and adaptation to new environments. An analysis of the potential function of 66 genes identified in nine reported cases of HGT between fungi showed a high representation of genes involved in nitrogen, amino acid, nucleic acid, protein, carbohydrate, and lipid metabolism, with cellular transport being the most prevalent putative function (Richards 2011). The acquisition of transporter-encoding genes is likely to be advantageous, as these genes may function to allow fungi to colonize new environments and utilize previously inaccessible nutrient sources.

Multiple recent HGTs have been reported in man-made environments and food processing chains (Borneman et al. 2008; Novo et al. 2009; Fitzpatrick 2011; Cheeseman et al. 2014). These ecological niches impose novel and stressful environments that exert strong selective pressure on microorganisms such as fungal pathogens, food contaminants, and the domesticated fungi used in beverages and food. The recent transfer of a huge (575 kb) genomic island, called Wallaby, between cheese-associated *Penicillium* species has recently been reported (Cheeseman et al. 2014). The function of the predicted 250 genes transferred suggests that some of them are involved in competition between microorganisms. Another striking example of HGT associated with domestication is the occurrence of multiple gene transfers from evolutionarily distant yeasts in the genome of *Saccharomyces cerevisiae* wine yeast (Novo et al. 2009). Three large genomic regions encompassing 39 genes (including five pseudogenes) and encoding functions potentially important for winemaking, such as sugar and nitrogen metabolism, have been found in *S. cerevisiae* (Novo et al. 2009). One of these regions was acquired from *Zygosaccharomyces bailii*, a distantly related species frequently found in wine environments as a contaminant. In many strains of *S. cerevisiae*, several copies of this region were found in different chromosomal locations, suggesting that a circular episome is involved in the transfer from *Z. bailii* to a recipient *S. cerevisiae* strain (Borneman et al. 2011; Galeote et al. 2011). Another independent event led to the acquisition, from an as yet unidentified yeast species, of a

Open Access

Article

65-kb subtelomeric region in EC1118 chromosome XV called region C (Novo et al. 2009). This region carries 19 genes, including *FSY1*, which encodes a high-affinity fructose/H^+ symporter that may be advantageous at the end of grape fermentation, when fructose is the most abundant sugar (Galeote et al. 2010). Two tandem duplicated genes—*FOT1–2*, encoding oligopeptide transporters—were also acquired, increasing considerably the number of di/tripeptides transported by this strain (Damon et al. 2011). However, the functional and ecological impacts of these events have not yet been demonstrated.

Despite a high number of documented HGT cases, there is a lack of functional evidence demonstrating the evolutionary advantage and biological relevance of HGT, preventing the evaluation of the importance of this process in the evolution of eukaryotic genomes (Ros and Hurst 2009; Schonknecht et al. 2014). In very few instances, the adaptive advantage of HGT genes in eukaryotes has been experimentally demonstrated, in most cases for single gene transfers of prokaryotic origin. A well-known example is the HGT of a bacterial gene encoding an oxygen-independent form of dihydroorotate dehydrogenase (*DHOD*) involved in the synthesis of uracil in Saccharomycetaceae, whereas the ancestral gene encoding a strict aerobic mitochondrial enzyme was lost in *Saccharomyces* sensu stricto species. Thus, this HGT was an important step in allowing these yeasts to grow in low-oxygen environments (Gojkovic et al. 2004; Hall et al. 2005).

Here, we report that *Torulaspora microellipsoides* is the donor of a large genomic region (region C) of between 65 and 80 kb in length found in *S. cerevisiae* wine yeast and closely related strains. Although the structure and number of genes present on this genomic island vary between wine strains, two tandem-duplicated *FOT1–2* genes encoding oligopeptide transporters are strongly conserved. We show that these genes confer a competitive advantage to wine yeast by increasing the amount and nature of nitrogen sources (oligopeptides) transported from grape must. These results highlight the existence of recurring eukaryote-to-eukaryote transfers between species sharing an ecological niche and constitute the first clear evidence of HGT-mediated adaptation of wine yeast to the nutritional challenges faced during wine fermentation.

Results

On the Origin of Region C

The origin of region C, a large genomic region of 65 kb in size initially found in the genome of the commercial *S. cerevisiae* wine strain EC1118 and carrying 19 genes (supplementary table S1, Supplementary Material online), has not been elucidated (Novo et al. 2009). We assayed for the presence of region C by polymerase chain reaction (PCR) amplification and sequencing of genomic segments of 187 strains from different genera belonging to the *Saccharomyces* complex (Kurtzman 2003). An analysis of these sequences indicated that *T. microellipsoides* might be the donor of region C. We therefore performed the sequencing and assembly of the whole genome of the *T. microellipsoides* type strain CLIB830^T. Mapping of the EC1118 region C to this genome enabled the identification of one scaffold of *T. microellipsoides* (fig. 1). This scaffold exhibits 99.5% shared identity with region C, which reaches 99.9% if we exclude two small regions of 1,400 and 2,150 bp with substantially lower identity (97.3% and 91.7% respectively) than the rest of region C (supplementary fig. S1, Supplementary Material online). Several hypotheses, exposed later, may explain the higher diversity of these two regions, encompassing *FOT1* gene (6502g) and on the other hand *ATO3*-like (6568g).

We found that the entire region C was present in *T. microellipsoides*. Moreover, *T. microellipsoides* carries an additional 93-kb region containing 40 genes between the first and the second genes of region C (as described in EC1118). The first gene of the EC1118 region C was a truncated, 500-bp *ARB1*-like gene (6469g), whereas in *T. microellipsoides*, a complete 1.8-kb *ARB1*-like gene was identified. This finding suggests an initial insertion of a 158-kb genomic fragment from *T. microellipsoides* into the *S. cerevisiae* genome followed by a loss of the 93 kb region. Phylogenetic analysis of each protein encoded by genes of the EC1118 region C (supplementary fig. S2A–O, Supplementary Material online) shows that most proteins cluster together with homologs from the *Zygosaccharomyces/Torulaspora* clade, supporting a transfer from *T. microellipsoides* to *S. cerevisiae*. However, few proteins (Hxt13, Gal10, Ato3, Fre7, and Sor1) clustered more closely than expected to *Saccharomyces* homologs. In these latter cases, they clustered with homologs from only few

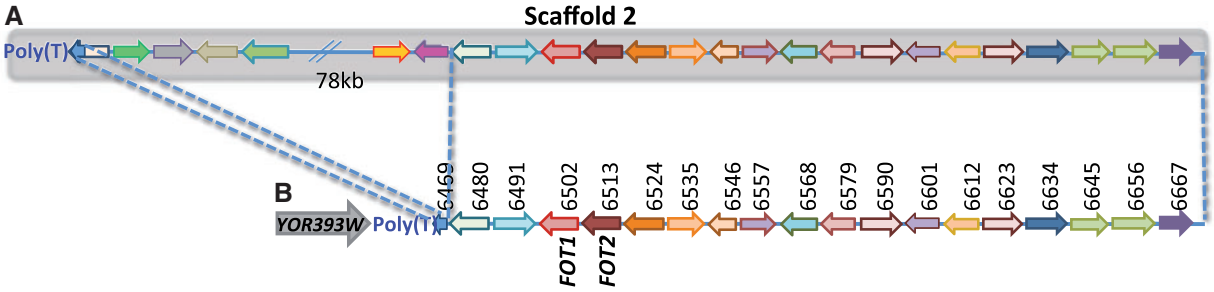

FIG. 1. Schematic representation of region C in *Saccharomyces cerevisiae* EC1118 and *Torulaspora microellipsoides* CLIB830 strains. (*A*) Physical mapping of the scaffold of CLIB830 carrying the different genes of region C. (*B*) The 19 genes of region C of *S. cerevisiae* EC1118 strain. Colored arrows represent syntenic ORFs, numbered according to Novo et al. (2009).

Saccharomyces species which refutes the hypothesis that these genes are originated from this clade. The observed topology could be explained by a complex evolutionary history of these genes, as suggested by the higher divergence observed above between the EC1118 and *T. microellipsoides ATO3* gene which may attest that this gene is evolving rapidly. Alternatively, this topology could be explained by other but more ancient HGT events associated with a pattern of gain and loss across species leading to a complex phylogeny. Such a turbulent evolutionary history has recently been described for *FSY1* found in region C (Coelho et al. 2013). The lack of genome sequences of other species closer to *T. microellipsoides* could be also another plausible explanation to the obtained topologies.

Evolutionary History of Region C in *S. cerevisiae*

We previously reported that regions A, B (from *Z. bailii*), and C (from *T. microellipsoides*, this study) are frequently found in wine yeasts and mosaic strains but only rarely in other lineages, suggesting that their acquisition is related to the early stages of wine domestication (Novo et al. 2009). In a previous study based on a limited number of available low-coverage genomes (39), region C was suggested to be incomplete in several wine strains (Novo et al. 2009). We therefore systematically analyzed 134 available genomes of *S. cerevisiae* from different ecological niches (wine, flor, rum, sake, palm wine, oak, bread, laboratory, clinical isolate, etc.; see supplementary table S2, Supplementary Material online, for strain list) for the presence of the 19 region C genes using BLASTN. This survey identified 36 strains containing at least one gene from region C, including 23 of 45 wine strains.

We selected 25 high-coverage genomes carrying this region for further analysis. Region C was fully conserved in 50% of the strains and partially conserved in the other half (fig. 2). Most strains that have a partially conserved region C have conserved only the four first genes, putatively encoding an ATPase (*ARB1*-like, 6469g), a transcription factor (6480g), an allantoate permease (*SEO1*-like, 6491g), and one copy of *FOT*. Interestingly, three strains (VIN13, K1-28, and 20B2) have lost all genes from this region except for one *FOT* copy and a truncated *SEO1*-like gene. These data show a robust conservation of *FOT*, suggesting that this gene plays an important role during the winemaking process.

Sequence alignment of Fot1 and Fot2 proteins and of the single Fot copy (present in strains K1-28, 20B2, VIN13, MO1A, 22A4, M22, DB1373, Lava32_15, L1414, and D47-6) revealed a novel Fot protein that we named Fot3. A comparative analysis of the different *FOT* genes found in *S. cerevisiae* and *T. microellipsoides* shows 99.7% identity between *FOT2* and a *T. microellipsoides FOT* gene that was named *FOT2_TOMI*. In contrast, *FOT1*, *FOT2*, and the newly identified *FOT3* in *S. cerevisiae* have only 97.8%, 93.3%, or 98% identity, respectively, with the second copy of *T. microellipsoides FOT*, which was named *FOTX_TOMI*. Fot1 and Fot3 exhibit

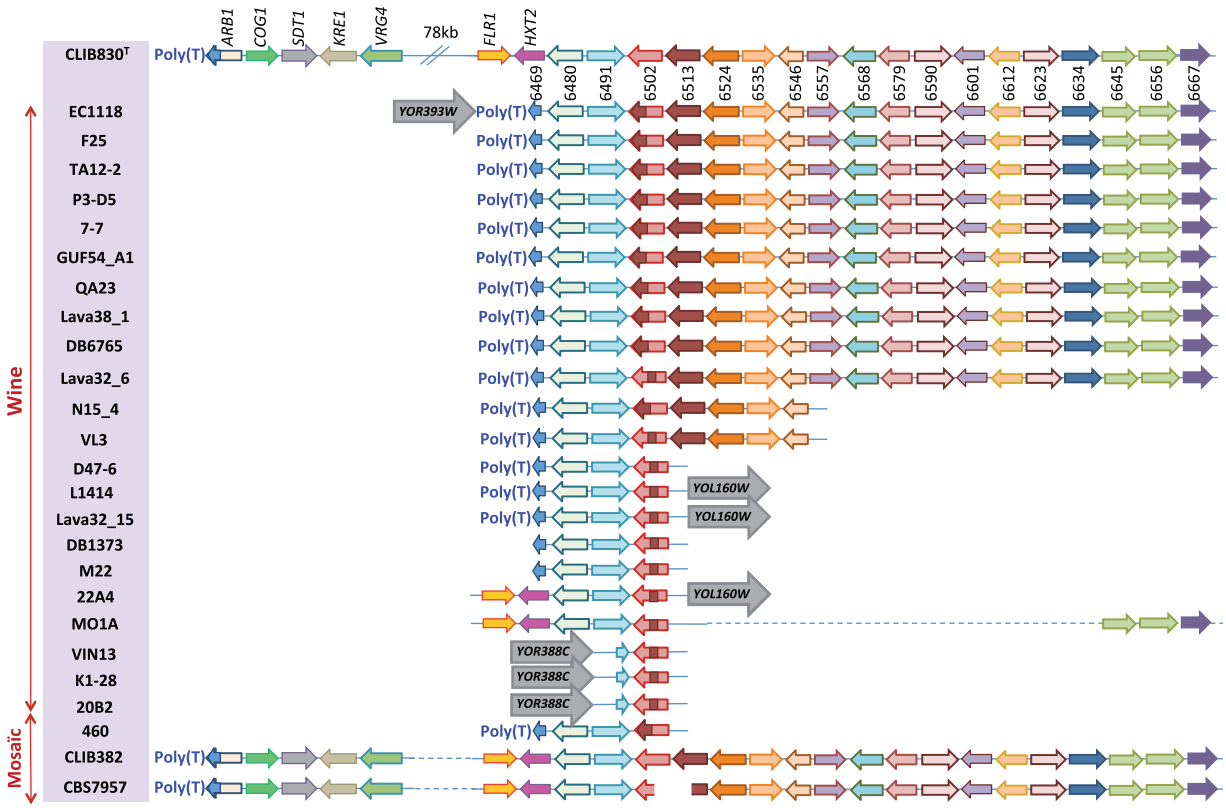

Fig. 2. Organization of region C in various strains. Colored arrows represent syntenic ORFs, numbered according to Novo et al. (2009), for *Saccharomyces cerevisiae* strains. *Torulaspora microellipsoides* predicted genes are assigned by sequence homology with *S. cerevisiae*. The chromosomal insertion positions are indicated by gray arrows.

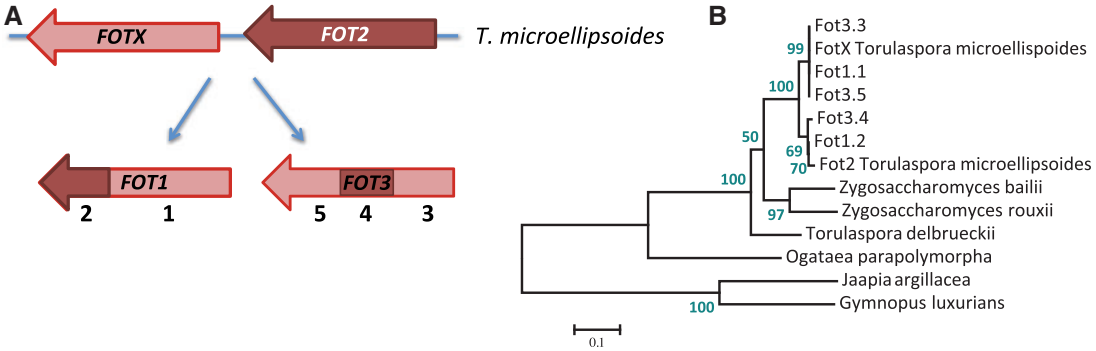

Fig. 3. Hypothetical formation of different *FOT* genes. (*A*) *FOT3* and *FOT1* may have been generated through two independent gene conversion events between *FOTX* and *FOT2*. (*B*) Phylogenetic relationships between protein sequences Fot 2 FotX, different parts of Fot1 and Fot3 (Fot1.1, Fot1.2, Fot3.3, Fot3.4, and Fot3.5 represented in part *A* of the figure), and their closest homologs searched using BLASTP in the National Center for Biotechnology Information and GRYC databases. Protein sequence alignment was performed with Muscle and visualized with Mega 5.2.2. Bootstrap values (percentage) based on 1,000 replicates are indicated at the nodes.

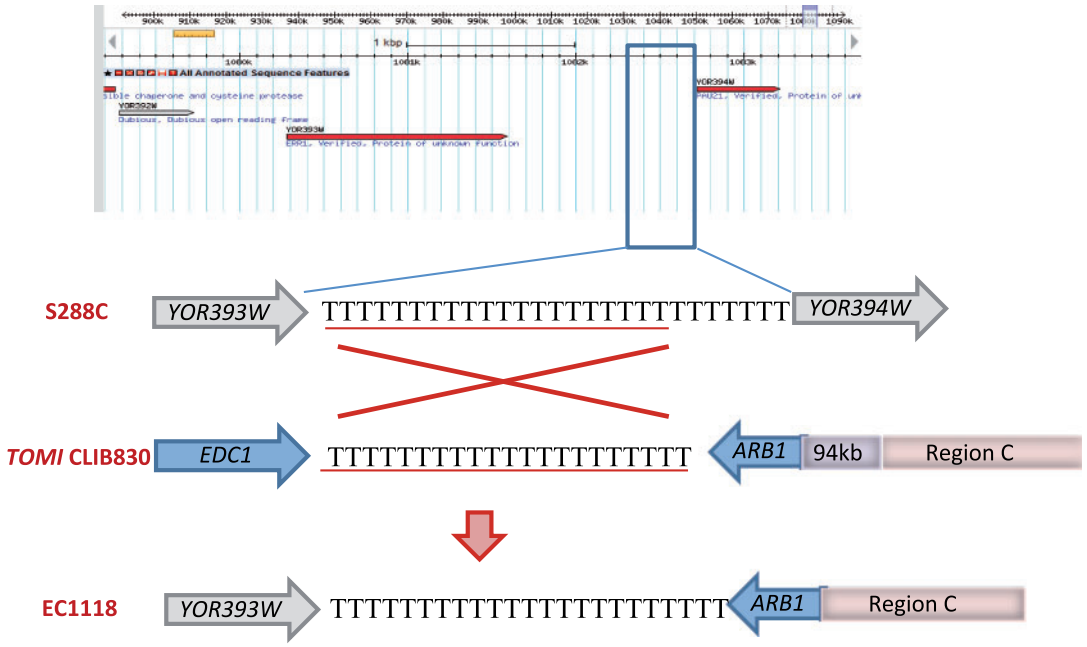

Fig. 4. Mechanism of insertion of region C by homologous recombination between poly(T) sequences located upstream of the region C in *Torulaspora microellipsoides* and downstream of *YOR393W* on *Saccharomyces cerevisiae* chromosome XV.

distinct composite amino acid patterns (supplementary fig. S3, Supplementary Material online), suggesting that both *FOT1* and *FOT3* are the result of two independent gene conversions between *FOTX_TOMI* and *FOT2_TOMI*, eventually accompanied by the independent loss of downstream regions (fig. 3*A*).

These results are supported by a phylogenetic tree showing the evolutionary relationships among the *FOT* genes (fig. 3*B*).

The location of region C (or the conserved portion of this region) differs according to strain (fig. 2). Strains 22A4, L1414, and Lava32_15 contain the four first genes of region C on chromosome XV, similar to EC1118 but on the left arm subtelomeric region instead of the right arm (confirmed by PCR analysis). In three other strains (K1-28, 20B2, and VIN13), this fragment is found five genes upstream of the insertion breakpoint in EC1118 (*YOR388C* instead of *YOR393W*, confirmed by PCR analysis). An analysis of the junctional sequence where region C is inserted into the genomes of the different strains revealed the presence of a poly(T) sequence (23–30 Ts) in the 14 strains possessing this region (fig. 2). Interestingly, we found a poly(T) sequence at the same locus in both S288C (27 Ts) and *T. microellipsoides* (21 Ts; fig. 4). This finding suggests that region C was inserted in the subtelomeric region of the chromosome XV of a recipient strain by homologous recombination between these poly (T) sequences.

We also identified in four strains (MO1A, 22A4, CBS7957, and CLIB382) a 7.3-kb-long sequence extension of region C immediately upstream of the second gene (*PUT3*-like) that was also present in the *T. microellipsoides* genome. Two open reading frames (ORFs) encoding a probable fluconazole resistance protein and a hexose transporter were identified in this fragment. In addition, we identified a 7.4-kb contig

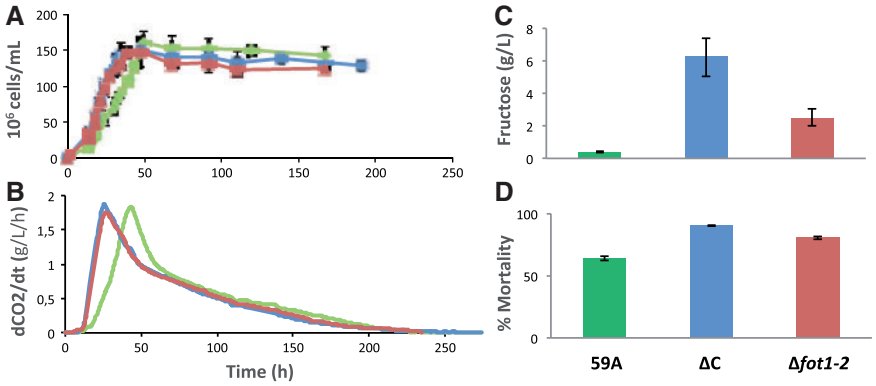

FIG. 5. Phenotypic analysis of 59A (green), ΔC (blue), and Δ*fot1–2* (red) in Chardonnay must. (*A*) Growth rate, (*B*) fermentation rate, (*C*) residual fructose measured at the end of fermentation ($t = 236$ h), and (*D*) mortality at the end of fermentation ($t = 236$ h); 59A. Data presented in (*A*), (*C*), and (*D*) are means ± SD ($n = 3$). A representative experiment is presented for (*B*).

encompassing five genes, with 99.9% of similarity to the upstream part of the 93-kb region identified in the genome of *T. microellipsoides*, in CBS7957 and CLIB382 strains. These five ORFs encode a putative complete ATP-binding protein Arb1-like, a Cog1 protein involved in protein trafficking, a pyrimidine nucleotidase Sdt1, a killer toxin resistance protein Kre29-like, and a Golgi GDP-mannose transporter Vrg4-like. The presence of these proteins suggests that the large genomic fragment of 158 kb was initially transferred to a recipient *S. cerevisiae* strain closely related to CLIB382 with a mosaic genome (Schacherer et al. 2009; Cromie et al. 2013) or to CBS7957, which exhibits close evolutionary relationships with the latter strain (supplementary fig. S4, Supplementary Material online).

These results indicate that region C has undergone many chromosomal rearrangements through gene conversion as well as gene losses following its acquisition from the donor yeast. In all cases, *FOT* genes were highly conserved among wine yeasts, suggesting that their presence confers a strong adaptive advantage in this environment.

The Effect of *FOT* Genes on Biomass, Viability, and Grape Must Fermentation

To investigate whether region C and *FOT* genes can confer an advantage upon exposure to the selective conditions of grape must fermentation, we deleted either the entire region C or the two tandem-duplicated genes *FOT1–2* in the wine yeast 59A, a haploid derivative of the EC1118 strain (Ambroset et al. 2011). During fermentation in a synthetic medium simulating a grape must, the wild-type and deletion mutants exhibited similar growth, fermentation rates, and metabolite profiles (data not shown). We therefore assessed the role of the *FOT* genes in a Chardonnay grape must containing more diversified nitrogen resources (e.g., γ-aminobutyric acid, peptides, or proteins) in addition to ammonium and amino acids. Although the deletion mutants showed superior growth and fermentation rates during the first hours of fermentation (fig. 5*A* and *B*), these advantages depreciated very quickly, resulting in an 8% and 12% lower biomass production in ΔC (183 mg/l, $P = 0.04$) and Δ*fot1–2* (270 mg/l, $P = 0.07$) mutants, respectively, compared with the wild-type. Furthermore, the deletion mutants exhibited a higher mortality rate by the end of fermentation (25% and 18% higher for ΔC and Δ*fot1–2*, respectively, compared with the wild-type strain) and performed incomplete fermentations, with 6 g/l of residual fructose for ΔC and 2.5 g/l for Δ*fot1–2* (fig. 5*C* and *D*). Thus, our data suggest that region C, and particularly the *FOT1–2* genes, plays a key role in maintaining cell viability and fermentation efficiency during the last step of wine fermentation. Nitrogen is the main limiting nutrient during wine fermentation. Its availability is directly related to biomass production, which governs the fermentation rate (Varela et al. 2004). As a consequence, nitrogen deficiency is the most prevalent cause of stuck and sluggish fermentations. As *FOT* genes encode transporters of a broad range of oligopeptides (Damon et al. 2011), the phenotypic differences between the wild-type and Δ*fot1–2* strains may result from a higher uptake by 59 A of nitrogen sources, such as small peptides.

Effect of *FOT* Genes on the Uptake of Oligopeptides

To evaluate the amount of oligopeptide in grape must, we purified the oligopeptide fraction less than 1 kDa, which includes small peptides of two to nine amino acids. This oligopeptide fraction (<1 kDa) represents a substantial part of the total nitrogen available in the grape must (17%), and approximately 10% of the total assimilated nitrogen. We then determined the total content of nitrogen, free amino acids, and oligopeptides in the grape must and in the wine fermented by the wild-type and mutant strains at the beginning of the stationary phase (40 g/l of CO_2 produced, after the nitrogen source was totally exhausted). Although all strains consumed the same amount of free amino acids and ammonium, 59A consumed approximately 35% more oligopeptide-derived nitrogen than the deletion mutants (~10 mg/l, $P = 0.027$ and 7.7 mg/l, $P = 0.037$ more than Δ*fot1–2* and ΔC, respectively). This difference is in agreement with the measured difference in biomass between the wild-type strain and the deletion mutants.

An analysis of the amino acid composition of the oligopeptide fraction of the grape juice shows that it is mainly composed of glutamate or glutamine (these two compounds are indistinguishable; table 1). The oligopeptide fraction consumed by 59A was particularly rich in glutamate/

glutamine and to a lesser extent in several other amino acids (fig. 6).

Because glutathione is a tripeptide composed of L-glutamate, L-cysteine, and glycine, which can be found in grape must in amounts ranging from 0 to 100 mg/l (Cheynier et al. 1989; Kritzinger et al. 2013), we also quantified this compound. In *S. cerevisiae*, glutathione is involved in many cellular processes, such as redox homeostasis and response to oxidative stress, and can also be used as a source of nitrogen and sulfur. We found that most glutathione in grape must supernatant is in the form of oxidized glutathione (GSSG; 16 mg/l vs. less than 2 mg/l reduced glutathione, GSH). The wild-type strain consumed more GSSG than deletion strains (fig. 7A). Furthermore, the wild-type strain grew better on SD medium supplemented with glutathione as the sole nitrogen source than the deletion mutant, which suggests that Fot1–2 is also able to transport glutathione (fig. 7B). Therefore, the consumption of glutathione contributes to the formation of a higher amount of biomass, even if the extra amount of nitrogen from glutathione consumed by 59A does not exceed 2 mg/l (corresponding to assimilation of 20% of the oligopeptides rich in glutamate/glutamine by Fot1–2).

Table 1. Amino Acid Composition of the Oligopeptide Fraction (<1 kDa) of the Chardonnay Must.

Amino acid	mg/l	mg N/l	μmol/l	%
Ala	0.519 ± 0.05	0.081 ± 0.008	5.83 ± 0.5	0.2
Arg	7.51 ± 2.7	2.41 ± 0.8	43.19 ± 15	1.7
Asp + Asn	12.31 ± 1.4	1.29 ± 0.14	92.58 ± 10	3.6
Glu + Gln	292.64 ± 3.9	27.87 ± 0.3	1,990.78 ± 26	77.3
Gly	12.48 ± 0.6	2.33 ± 0.1	166.44 ± 8	6.5
His	4.14 ± 1.2	1.12 ± 0.34	26.77 ± 8	1.0
Ile	1.34 ± 0.1	0.144 ± 0.03	10.30 ± 2	0.4
Leu	4.09 ± 0.4	0.437 ± 0.05	31.25 ± 3	1.2
Lys	3.88 ± 0.3	0.744 ± 1.9	26.57 ± 2	1.0
Phe	1.88 ± 0.4	0.159 ± 0.04	11.42 ± 2.8	0.4
Ser	6.54 ± 1.1	0.873 ± 0.1	62.36 ± 10	2.4
Thr	6.23 ± 1.3	0.733 ± 0.1	52.39 ± 11	2.0
Tyr	6.52 ± 1.4	0.504 ± 0.1	36.05 ± 8	1.4
Val	2.43 ± 1	0.291 ± 0.1	20.80 ± 8	0.8

NOTE.—N, assimilable nitrogen.

FOT1–2 Genes Increase Strain Fitness during Wine Fermentation

To evaluate the adaptive role of *FOT* genes, we performed competition experiments under controlled wine fermentation

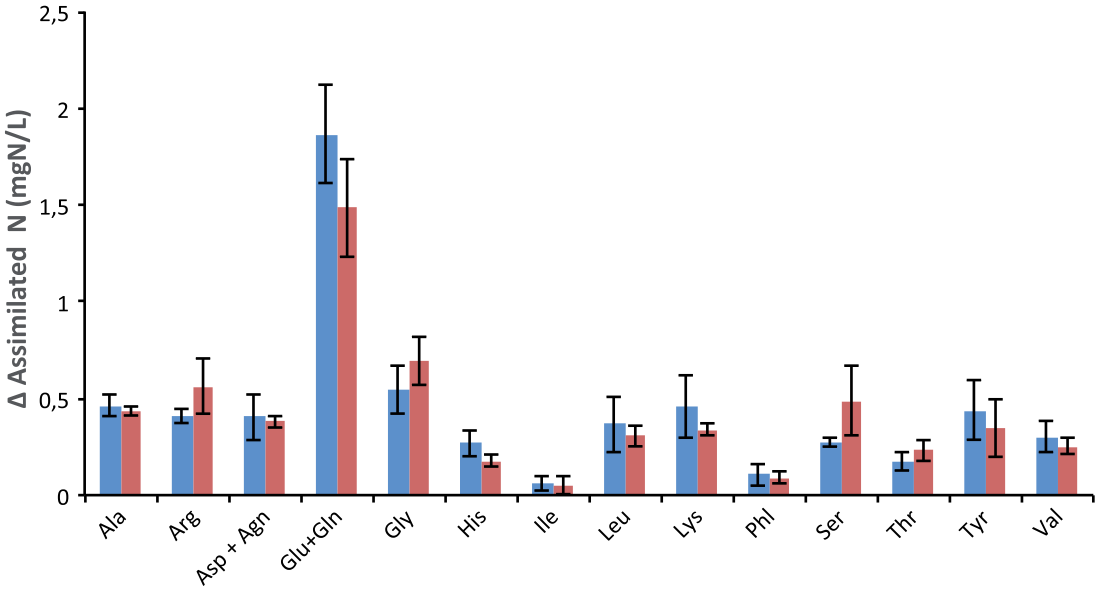

FIG. 6. Amino acid composition of the oligopeptide fraction of the Chardonnay must specifically assimilated by 59A in comparison with ΔC (blue) or Δ*fot1–2* (red) strains at the beginning of the stationary phase (40 g/l of CO_2 production). Data are presented as means ± SD ($n = 3$).

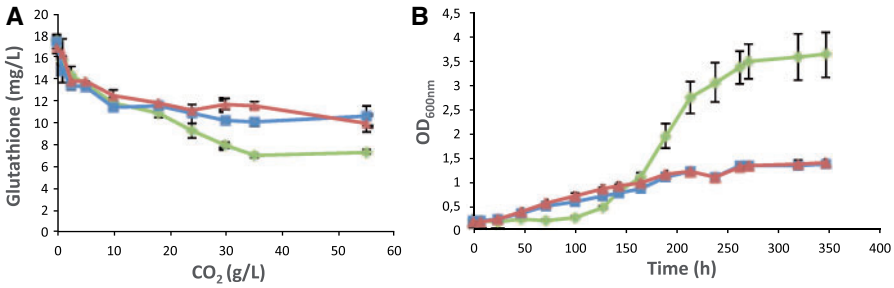

FIG. 7. (*A*) Consumption of glutathione during grape must fermentation and (*B*) growth in SD medium containing glutathione as the sole nitrogen source; 59A (green diamond), ΔC (blue square), and Δ*fot1–2* (red triangle). Data are presented as means ± SD ($n = 3$).

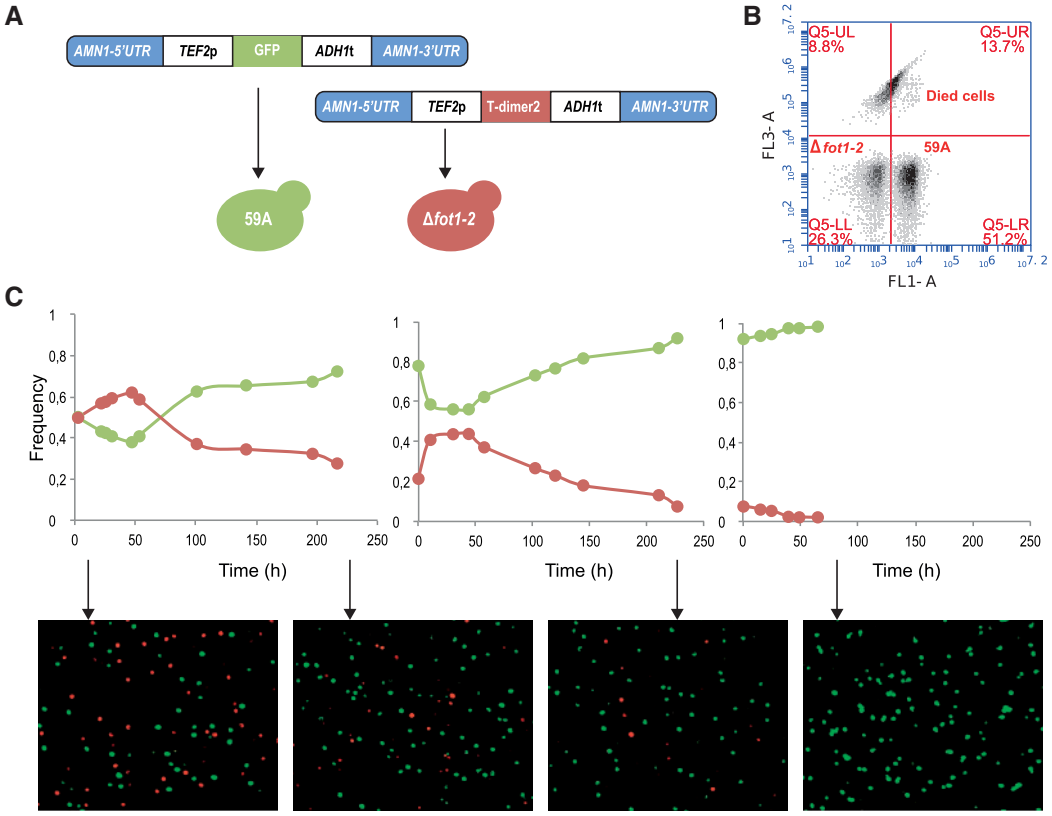

Fig. 8. Competition assay using 59A and Δ*fot1*–2 strains in Chardonnay grape must. (*A*) A GFP-labeled wild-type strain was grown in competition with a tdimer2-labelled Δ*fot1*–2 strain. (*B*) An example of separation of GFP-labeled wild-type and tdimer2-labelled Δ*fot1*–2 strains by flow cytometry. (*C*) Three successive fermentations in Chardonnay grape must were performed, and the frequency of 59A-GFP (green) and Δ*fot1*–2-tdimer2 (red) cells was monitored by flow cytometry throughout the fermentation. Cells were also observed by microscopy at the time points indicated by arrows.

conditions. Cocultures of 59 A expressing green fluorescent protein (GFP) and *FOT1*–2 mutant yeast expressing red fluorescent protein (t-dimer2) (fig. 8*A*) were achieved during three successive fermentation experiments on grape must. The relative abundance of each strain was monitored over time by flow cytometry (fig. 8*B*). These competition assays revealed a considerable competitive advantage of the strain with *FOT* genes in natural must. Despite a transient advantage of the deletion mutant during the early steps of fermentation, which is in line with its higher growth and fermentation rates at this stage, the Δ*fot1*–2 strain was quickly dominated during the stationary phase (fig. 8*C*). At the beginning of the third successive coculture, the *FOT1*–2 mutant completely disappeared from the coculture (fig. 8*C*). We verified that these results were not biased by the use of different fluorescent proteins and that the presence of these fluorochromes did not affect the fitness of the strains. These results demonstrate the strong selective advantage provided by *FOT1*–2 genes during wine fermentation.

Discussion

Saccharomyces cerevisiae wine yeasts have been used for winemaking for several millennia and display outstanding fermentative capacities. During wine fermentation, these yeasts are challenged with various stresses, including high sugar content, low pH, the presence of ethanol and sulfites, and long periods of nutrient starvation, which have prompted their adaptive evolution.

In this study, we identified *T. microellipsoides* as the donor of the large 65-kb genomic region previously characterized in the genome of *S. cerevisiae* wine yeasts (Novo et al. 2009). The high identity (99.9 %) of the regions found in these two distant species of the Saccharomycetaceae family indicated a recent transfer event. In addition, the maximum divergence within a conserved 9-kb fragment of the region C containing the first three genes (*ARB1*, *PUT3*, and *SEO1*) between 12 wine strains is very low, about 0.2 nucleotidic difference per kilobase. Considering that vine and yeast domestication occurred during Neolithic era (~9,000 years ago) (McGovern et al. 2004; Fay and Benavides 2005; Legras et al. 2007) and that divergence between wine strains is about 1.0 nucleotidic difference per kilobase (Fay and Benavides 2005; Liti et al. 2009), we can estimate that this HGT event occurred more recently than 2,000 years ago. This region is present in the genomes of many wine strains as well as few mosaic strains, including two evolutionarily related strains that are closest to the donor, as shown by the presence of an additional larger *T. microellipsoides* block in their genomes. The genome of one of these strains, CLIB382, was shown to have a major contribution from the wine group (Schacherer et al. 2009). A plausible scenario is the transfer of a large genomic fragment (158 kb) from *T. microellipsoides* to a recipient *S. cerevisiae* strain, likely introgressed by a rare unstable hybridization

(Marinoni et al. 1999), followed by the spreading of this region among wine strains by outcrossing. During this process, this region underwent several rearrangements, including gene losses and gene conversion through *FOT* genes, resulting in a patchy distribution among various strains. Except for *FOT* genes, which were found in all strains, other parts of the *T. microellipsoides* region were not universally present, suggesting that they may have been lost because they did not contribute new or important functions. Interestingly, novel *FOT* alleles with potentially specialized functions were generated by gene conversion, which supports the view of a selective advantage conferred by *FOT* genes.

We also report evidence that the presence of *FOT* genes, which substantially increases the number and the diversity of oligopeptides that yeast can utilize from grape must, confers a strong adaptive advantage to wine strains. In the Chardonnay must, Fot transporters preferentially assimilate glutathione and oligopeptides rich in glutamate/glutamine, which are the most abundant amino acids comprising the oligopeptide fraction (<1 kDa). Yokotsuka and Fukui (2002) recently found that the proteins of berries from six different grape cultivars, including Chardonnay, are rich in aspartic acid and glutamate/glutamine, suggesting that active *FOT* transporters might be advantageous during the fermentation of must from a diverse variety of grapes.

It is noteworthy that *S. cerevisiae* already possesses various oligopeptide transporters, including Ptr2 and Dal5, which can transport di- and tripeptides (Homann et al. 2005; Cai et al. 2007), and Opt1 and Opt2, which can transport oligopeptides of 4–5 amino acids in length as well as glutathione (Bourbouloux 2000; Aouida et al. 2009). However, the major di/tripeptide transporter, Ptr2, has a low affinity for negatively charged amino acids such as glutamate and aspartate and for amino acids predicted to influence peptide bond conformation such as glycine and proline (Ito et al. 2013). We previously showed that the strain 59A transports a considerably higher number of dipeptides and tripeptides than the Δ*fot1–2* mutant (118 vs. 28) and than a laboratory strain with only the *PTR2* and *DAL5* transporter genes (Damon et al. 2011). Among the dipeptides specifically used by 59A but not by the laboratory strain, five contained one glutamate and two contained aspartate—two amino acids absent from the dipeptides transported by the laboratory strain (Damon et al. 2011). These data support our findings that the *FOT1–2* genes confer a strong advantage to yeast grown in grape must rich in glutamate/glutamine oligopeptides and indicate a specific adaptation to the wine environment.

Competition experiments demonstrate a strong competitive advantage conferred by the acquisition of *FOT1–2* genes, as Δ*fot1–2* mutants were completely outcompeted by the wild-type strain after three successive cocultures. The increased fitness provided by the *FOT* genes might result from both the higher biomass and the higher viability of 59A during the stationary phase. Although the higher biomass formation is the consequence of greater nitrogen assimilation, the superior viability might be linked to the quality of assimilated oligopeptides. Interestingly, the presence of Fot1–2 increases the assimilation of glutathione, an essential metabolite that protects cells against oxidative stress and aging. Glutathione protects cells from the deleterious effects of reactive oxygen species (ROS), which may cause oxidative damage to proteins, nucleic acids and lipids as well as other cellular components, and may lead to cell death (Lee et al. 2001). Strains with disruptions in genes involved in glutathione biosynthesis have a reduced tolerance to a wide range of stress conditions and undergo apoptosis at a high rate compared with the wild-type strain (Grant et al. 1998; Madeo et al. 1999). Conversely, exogenous administration of glutathione rescues the higher mortality of *S. cerevisiae* strains in the presence of oxygen (Nestelbacher et al. 2000). During wine fermentation, ROS may be part of the cellular response to a variety of stressors (Gibson et al. 2008; Landolfo et al. 2008). In particular, nitrogen depletion induces ROS accumulation during must fermentation, causing cell membrane damage and cell cycle arrest in G0/G1 and inducing autophagy (Mendes-Ferreira et al. 2010). Therefore, the higher viability of strains with *FOT1–2* genes in grape might be explained, at least partly, by the greater assimilation of glutathione. Glutamate may also play an important role in maintaining cell viability and in tackling oxidative stress. The $NADP^+$-dependent glutamate dehydrogenase Gdh3 plays a role in resistance to stress-induced apoptosis in the stationary phase (Lee et al. 2012). Indeed, *S. cerevisiae gdh3* mutants rapidly lose viability, are depleted in glutathione and accumulate ROS during the stationary phase.

Overall, this study supports a major role for HGT in the evolution of wine yeast genomes. Membrane transporters are one functional category of gene more prone to horizontal transfer and to evolution by duplication (Richards 2011; McDonald et al. 2012). This plasticity may be linked to the important roles that transporters can play in detoxification processes or in providing a competitive advantage in the struggle for nutrients (Richards 2011; Richards and Talbot 2013). In fact, it is important for osmotrophs such as fungi to acquire nutrients rapidly, thereby making public goods inaccessible to others (Richards and Talbot 2013). Several other cases of HGT involving high-affinity transporters have been reported and likely reflect adaptation to these pressures (Slot and Hibbett 2007; Galeote et al. 2010; Coelho et al. 2013).

Overall, the origin of the *T. microellipsoides* region C is reminiscent of the *Z. bailii* origin of region B, which is also widespread in the genome of wine yeasts. *Torulaspora microellipsoides* and *Z. bailii* are closely related to a food and beverage spoilage-yeast cluster (Steels et al. 1999). These species are isolated from various fruit juices, soft drinks, and beverages, including wine (Deak 2007; Kurtzman 2011). Interestingly, it has been reported that *ASP3*, a *S. cerevisiae* gene induced by nitrogen starvation, was likely acquired by HGT from *Wickerhamomyces anomalus*, a distant yeast species used in a variety of biotechnological applications (League et al. 2012). Asp3 can hydrolyze D-asparagine (Dunlop et al. 1978) and is also involved in the utilization of dipeptides with C-terminal asparagine residues (Homann et al. 2005). A high diversity in the capacity of *S. cerevisiae* strains of various origin to utilize di- and tripeptides as nutrient sources has been highlighted previously (Homann et al. 2005). The presence

of the *ASP3* and *FOT* genes might contribute to this phenotypic diversity.

The finding of recurrent transfers in food (Novo et al. 2009; League et al. 2012; Cheeseman et al. 2014) suggests that man-made environments offer ecological opportunities for sharing metabolic genes between distant yeasts. These HGT processes may help yeast to evolve to survive fluctuations in the external environment by adapting their metabolic networks to meet the challenges of their ecological niche. In line with this hypothesis, we found that *FOT* genes facilitate the utilization of the nitrogen resources in grape must, which are present in limiting amounts in grape juice. Nitrogen is a key nutrient consumed at the beginning of the fermentation process, and its deficiency can lead both to sluggish and stuck fermentations (Blateyron and Sablayrolles 2001). It is noteworthy that several of the transferred genes gained by the acquisition of the three non-*Saccharomyces* regions identified in wine yeasts (Novo et al. 2009) have putative functions related to nitrogen metabolism, including an asparaginase, an oxoprolinase, an ammonium transporter, an allantoate transporter, and two transcription factors related to the biosynthesis enzymes involved in lysine and proline utilization. This study strongly supports the view that HGT plays an important role in the adaptation of fungi to their environments and that these events are favored in the ecological niches created by food and beverages, where many yeast species cohabit. As a consequence, a better knowledge of the functional and ecological impacts of HGT also increases our understanding of the unintentional domestication of wine yeasts through elucidating the genetic bases of yeast strain adaptation to specific ecological niches.

Materials and Methods

Yeast Strains and Fermentation Conditions

The *S. cerevisiae* strain 59A is a haploid derivative of the commercial wine strain EC1118 (Ambroset et al. 2011). The recombinant strains constructed and used in this study are listed in table 2. Fermentations were performed in synthetic medium, which mimics a natural grape must (Bely et al. 1990) and contains 200 g/l glucose/fructose, 425 mg/l assimilable nitrogen contained in a mixture of amino acids and ammonium, 1.12 mg/l oleic acid and 3.75 mg/l ergosterol, pH 3.3. For a natural grape must, we used a Chardonnay (Coursan, France 2012) containing 230 g/l of sugars (100 g/l glucose and 130 g/l of fructose) and 240 mg/l of yeast assimilable nitrogen (free amino acids and ammonium).

Fermentation experiments were performed in 1.2-l fermenters inoculated at a density of 10^6 cells/ml. Yeast cells were first grown overnight at 28 °C in 10-ml flasks containing YPD (1% Bacto yeast extract, 2% bactopeptone, 2% glucose) with shaking (180 rpm) and were transferred to 20-ml flasks containing the grape must for 24 h. These precultures were used to inoculate fermenters equipped with airlocks to maintain anaerobiosis, and fermentations were performed at 24 °C with constant magnetic stirring (150 rpm). The CO_2 released was estimated by an automatic measurement of the weight loss of the fermenter every 20 min, and the rate of CO_2 production was calculated by polynomial smoothing of the CO_2 released (Sablayrolles et al. 1987).

Strain Construction

Deletion of the 65-kb region C was performed by four successive deletions of 8- to 21-kb fragments. Each fragment was replaced by the loxP–KanMX4–loxP deletion module using the short-flanking homology PCR technique (Schiestl and Gietz 1989). The KanMX4 cassette was PCR amplified from the pUG6 vector using the primers listed in table 3. The PCR fragments were used to transform 59A using the lithium acetate method (Güldener et al. 1996). The deletions were verified by PCR analysis of total DNA isolated from kanamycin-resistant transformants, using primers flanking the deleted regions. After each deletion, we used the *Cre-loxP* recombination system for marker rescue (Güldener et al. 1996). The deleted strain was transformed with the *cre* expression plasmid pSH65, which carries the phleomycin marker gene and the *cre* gene under the control of the inducible *GAL1* promoter. Cells were plated on YPM medium containing maltose (2%) to induce expression of the *Cre* recombinase. The plasmid was then removed by streaking cells on YPD without phleomycin. Deletion of the two tandem duplicated *FOT1–2* genes was obtained by replacing the two ORFs with the *loxP–KanMX–loxP* module using the custom primers listed in table 3.

Because strain 59A forms aggregated cells in liquid culture, which causes problems in cell counting and flow cytometry applications, we deleted the *AMN1* gene, which encodes a protein required for daughter cell separation and is involved in cell aggregation (Wang et al. 2003; Yvert et al. 2003). Deletion of *AMN1* in 59A, ΔC, and Δ*fot1–2* strains was performed as described above using primers listed in table 3.

For competition experiments, the wild-type and Δ*fot1–2* strains were tagged with the fluorochromes GFP and t-dimer2, respectively. To this end, a cassette containing

Table 2. Strains Used and Constructed in This Study.

Strain	Genotype	Source
59A	MATa ho	Ambroset et al. (2011)
Δ*amn1*	MATa ho *AMN1*::kanMX4	This study
Δ*fot1–2*	MATa ho *FOT1–2*::loxP *AMN1*::kanMX4	This study
ΔC	MATa ho Region C::loxP; *AMN1*::kanMX4	This study
59A-GFP	MATa ho *AMN1*::TEF2Pr-GFP-ADH1-NATMX4	This study
Δ*fot1–2*-tdimer2	MATa ho *FOT1–2*::loxP *AMN1*::TEF2Pr-t-dimer2-ADH1-NATMX4	This study

Table 3. Primers Used in This Study.

Primer	Sequence
Δ*fot1–2*-F	5′-GGATTTCCGTCGTCCTGTGATGGCAACTGCCTTAGGCCACTTCGTACGCTGCAGGTCGC-3′
Δ*fot1–2*-R	5′-AAACTTCGACTAAAGCTTGTCGCAAATCCACGTAAACTAAGCATAGGCCACTAGTGGATCTG-3′
ΔC1-F	5′-CCTTTCGGATGATACTGCTTGGACATGGTACGCTTTAGAGTTCGTACGCTGCAGGTCGAC-3′
ΔC1-R	5′-GGTTCCTGCCTCTTCGTACTCAAATTGGCTACTGCATATTCGCATAGGCCACTAGTGGATCTG-3′
ΔC2-R	5′-GGGAGCTTGACTAGAAAGTCTTCGGGGGACAGGTAGTACTGCATAGGCCACTAGTGGATCTG-3′
ΔC3-R	5′-ATCTACGGAAACCGCGACTGTCTCCGGTGCCTGCCCAATAGCATAGGCCACTAGTGGATCTG-3′
ΔC4-F	5′-GTTCATCCAGTAGTAGAACATTGGGCTGCTCAAGGGCTAGTTCGTACGCTGCAGGTCGAC-3′
ΔC4-R	5′-TAACAGCCCATTCCATCCGCGTTTCGTTATGTACATGCCCGCATAGGCCACTAGTGGATCTG-3′
Δ*amn1*F	5′-TAATTTATCATTTTCCTTTTCTGTTAGTAAAGCACCCATTAAATGTTCGTACGCTGCAGGTCGAC-3′
Δ*amn1*R	5′-GGTCTGTTGTGTACTATTTATAGGTAAAGTCACAAAAACCATCTAGCATAGGCCACTAGTGGATCTG-3′
Fluo-F	5′-TAATTTATCATTTTCCTTTTCTGTTAGTAAAGCACCCATTAAATG*GGTCGACGGATCCCCGGGTT*-3′
Fluo-R	5′-GGTCTGTTGTGTACTATTTATAGGTAAAGTCACAAAAACCATCT*ATCGATGAATTCGAGCTCGTT*-3′

NOTE.—Homologous sequence to KanMx4 cassette of pug6 are underlined. Homologous sequence to clonNat cassette of pFA6a-TEF2Pr-GFP-ADH1-NATMX4 or pFA6a-TEF2Pr-t-dimer2-ADH1-NATMX4 are in italic.

the *TEF2* promoter, *GFP* or t-dimer2, the *ADH1* terminator, and a gene conferring resistance to clonNat was amplified by PCR using specific primers (Fluo-F and Fluo-R, table 3) and the previously described plasmids pFA6a-TEF2Pr-GFP-ADH1-NATMX4 or pFA6a-TEF2Pr-t-dimer2-ADH1-NATMX4 (Breslow et al. 2008) as templates. The amplified fragments were inserted into the *AMN1* locus, yielding strains 59A-GFP and Δ*fot1–2*-tdimer2.

Cell Population, Viability, and GFP Activity

Population size was determined by counting yeast cells with an electronic particle counter (Multisizer 3 coulter counter; Beckman Coulter, CA). Cell viability and GFP activity were determined by flow cytometry using a C6 cytometer (Accuri, BD Biosciences, Piscataway). Cell viability was analyzed by adding propidium iodide (PI) (Calbiochem, CA) to cell suspensions (5 µl of 0.1 mg ml^{-1} solution). PI is a fluorescent nucleic acid stain (excitation 488 nm, emission 575 nm) that penetrates nonviable cells with a damaged membrane. PI flow cytometry analysis was performed after 10 min of staining. Fluorescence data for cells stained by PI were collected in the FL3 channel. Mortality was defined as the percentage of dead cells among all cells. For GFP activity, fluorescence (excitation 488 nm, emission 530 nm) was collected in the FL1 channel.

Fluorescence Microscopy

Fluorescent cells tagged with GFP and t-dimer2 in coculture were visualized at the beginning and the end of fermentation of Chardonnay must. The microscope (Axio Imager Cam MRM A2, Carl Zeiss, New York) equipped with an excitation source and a range of filters for viewing fluorescent cells was used. For this study, the filter 38 (excitation BP 470/40 and emission BP 525/50) was used for cells tagged with GFP (488 nm excitation and 530 nm emission). The filter 20 (excitation: BP 546/12, emission: BP 575–640) was used for cells tagged with t-dimer2 (excitation 568 nm, 630 nm emission).

Analytical Methods

Residual fructose was analyzed by high-pressure liquid chromatography (HPLC 1100; Agilent Technologies, CA) on an HPX-87H Aminex column (Bio-Rad Laboratories Inc., CA). Dual detection was performed with a refractometer and a UV detector (Hewlett Packard).

The total nitrogen concentration was determined by distillation and back-titration according to the Kjeldahl mineralization method (Scheiner 1976). The residual ammonium concentration in the medium was measured by spectrophotometry using glutamate dehydrogenase (Enzytec fluid Ammonia; R-Biopharm, Darmstadt, Germany).

The oligopeptide fraction of the must was purified by two successive ultrafiltrations using a hollow fiber cartridge filter, UFP-10-C-4, to recover the peptides under 10 kDa followed by ultrafiltration using a hallow fiber cartridge filter, UFP-1-C-4, to recover oligopeptide fractions under 1 kDa. The oligopeptide purified fraction less than 1 kDa was then hydrolyzed by incubation for 24 h at 110 °C in 6N HCl. Upon hydrolysis, some amino acids are degraded. A part of cysteine and methionine are oxidized and degraded into H-cysteine and methionine sulfone. Tryptophan, sensitive to heat in an acid medium, is completely degraded and thus not determined. Similarly, the glutamine is converted to glutamate; measured glutamate corresponds to the concentration of glutamate and glutamine. This is also the case for asparagine which is converted to aspartate. Total amino acids were analyzed with a Biochrom 30 analyzer. Molecules with a high molecular weight were precipitated for 1 h at 4 °C and centrifuged (4 °C, 10 min, 3,000 × g). The sample was then filtered through a 0.22-µm pore-size Millipore nitrocellulose membrane. Amino acids were separated by liquid chromatography on an ion-exchange column (Ultra-pac-8 lithium form; Amersham Pharmacia Biotech, Piscataway) and revealed by the ninhydrin reaction, followed by absorbance measurements at 570 nm, except for proline, which was detected by measuring the absorbance at 440 nm. Norleucine (0.5 mmol/ml) was added to the samples and used as an internal standard. Total amino acids detected in the hydrolysates of

the extracts minus the free amino acids detected in the same extract before hydrolysis were classified as bound amino acids–oligopeptides. Glutathione consumption during must fermentation was also analyzed with the Biochrom 30 as described above.

Genome Sequence and Analysis

Of the 134 genomes studied, 77 were available in public databases and 57 were newly sequenced in our laboratory (Genowine and Evolya projects).

The 16 (Genowine) and 41 (Evolya) DNA samples were processed to generate libraries of short 400-bp inserts. After passing quality control, the libraries were sequenced using an Illumina HiSeq 2000 platform. Sequencing from both ends generated paired-end reads of 2 × 100 bp, resulting in sequencing depth of 70 to 700× (Genowine project) and 90 to 350× (Evolya project). The entire data sets were deposited in the European Nucleotide Archive (ENA) database under study accessions PRJEB6529 (Genowine) and PRJEB7675 (Evolya).

For the PRJEB6529 project, filtered reads were corrected for sequencing errors using Quake v0.3.0. Assembly and scaffolding were carried out using SOAPdenovo v1.05 software, fixing the max_rd_len parameter at 75 and selecting the k-mer lengths resulting in the highest N50 scaffold length. Gaps emerging during the scaffolding process were closed using GapCloser v1.10.

For the PRJEB7675 project, filtering of low-quality regions was performed with trimming if base quality dropped below Q20. Reads shorter than 30 bp were also removed. Assembly and scaffolding were carried out using Velvet v1.2.07 software, selecting the k-mer length resulting in the highest N50 scaffold length. Gaps emerging during the scaffolding process were closed using GapCloser.

Total DNA from the *T. microellipsoides* strain CLIB830^T was processed to generate two libraries: 1) A 500-bp insert length paired-end library and 2) a 6-kb insert length mate paired library. After passing quality controls, the libraries were sequenced using an Illumina HiSeq 2000 platform. Sequencing generated 2 × 100 bp reads per library, resulting in an average sequencing depth of 374×. The entire data set was deposited in the ENA database under study accession PRJEB7632.

Trimomatic v0.32 was used for cleaning and trimming low quality regions and adapters in Illumina data (Bolger et al. 2014). Read sequences were trimmed for the first and last three nucleotides. Filtering of low-quality regions was performed using a sliding window of 20 bp, cutting once the average quality within the window falls below a threshold of 25. Furthermore, reads shorter than 75-bp were further discarded.

In order to remove short inward reads contaminating the maite-pair library, reads were first mapped to the S288C reference genome with BWA v0.6.2 using default parameters (Li and Durbin 2010). Then inwards read pairs were removed using BamTools v2.2.3 "filter command" (Barnett et al. 2011). Picard v1.117 (http://broadinstitute.github.io/picard) "SamToFastq" command was then used to extract resulting reads from the BAM file.

Assembly and scaffolding were carried out using SOAPdenovo2 v2.04, using a kmer value of 61 and the following parameters: paired-end: pair_num_cutoff = 5, map_len = 32; maite-pair: pair_num_cutoff = 10, map_len = 50 (Luo et al. 2012). Closing gap was performed using GapCloser v1.12 using default parameters (Luo et al. 2012).

Reconstruction of the complete nucleotide sequence of the HGT region C of *T. microellipsoides* presents on scaffold2 was performed using targeted PCR and capillary sequencing of the resulting amplicons. This scaffold has been submitted to the ENA (accession number: LN811465).

Similarity search among the yeast genome sequences was performed using BLAST (Altschul et al. 1990).

The nucleotidic diversity of region C in EC1118 and *T. microellipsoides* has been calculated from the alignment of EC1118 and *T. microellipsoides* regions C with variscan software for 1-kb sliding windows separated by 200-bp steps.

Molecular Phylogenetic Analysis Using the Maximum-Likelihood Method

Protein sequences homologous to the each ORF of the region C protein were identified by a BLASTP search of the National Center for Biotechnology Information and GRYC (Genome Resources for Yeast Chromosomes http://gryc.inra.fr/index.php?page=home, last accessed March 16, 2015) databases. Amino acid sequences were aligned using MUSCLE. The evolutionary history was inferred by using the maximum-likelihood method based on the JTT (Jones, Taylor, and Thorton) matrix-based model (Jones et al. 1992) as proposed by MEGA5.2.2. software (Tamura et al. 2011). For each phylogeny, the tree with the highest log likelihood is shown. For each pairwise comparison, all sites covered are taken in account. The bootstrap value of 1,000 replicates is shown next to each node. Initial trees for the heuristic search were obtained by applying the neighbor-joining method to a matrix of pairwise distances estimated using a JTT model. The trees are drawn to scale, with branch lengths measured in the number of substitutions per site.

Accession Codes

Genome sequence data for *Saccharomyces cerevisiae* strains have been deposited in the European Nucleotide Archive (ENA) database under the accession codes PRJEB6529 (Genowine project) and PRJEB7675 (Evolya project). Genome sequence data for *T. microellipsoides* have been deposited in the European Nucleotide Archive (ENA) database under study accession PRJEB7632.

Supplementary Material

Supplementary figures S1–S4 and table S1 and S2 are available at *Molecular Biology and Evolution* online (http://www.mbe.oxfordjournals.org/).

Acknowledgments

This work was supported by grants GIS IBiSA-AO 2010-2011, France to S.D., V.G., J.L.L., and F.B.; AIP Bioressources from the National Institute for Agricultural Research, France to S.D., V.G., J.L.L., F.B.; and AGL2012-39937-C02-02 from the Spanish government to E.B. S.M. and A.M. acknowledge support by a doctoral grant and an FPI fellowship from the French and Spanish governments, respectively. They acknowledge Therese Marlin and Pierre Delobel for their help with the glutathione and flux cytometer analyses.

References

Altschul SF, Gish W, Miller W, Myers EW, Lipman DJ. 1990. Basic local alignment search tool. *J Mol Biol.* 215:403–410.

Ambroset C, Petit M, Brion C, Sanchez I, Delobel P, Guérin C, Chiapello H, Nicolas P, Bigey F, Dequin S, et al. 2011. Deciphering the molecular basis of wine yeast fermentation traits using a combined genetic and genomic approach. *G3* 1:263–281.

Andersson JO. 2009. Gene transfer and diversification of microbial eukaryotes. *Annu Rev Microbiol.* 63:177–193.

Aouida M, Khodami-Pour A, Ramotar D. 2009. Novel role for the *Saccharomyces cerevisiae* oligopeptide transporter Opt2 in drug detoxification. *Biochem Cell Biol.* 87:653–661.

Barnett DW, Garrison EK, Quinlan AR, Stromberg MP, Marth GT. 2011. BamTools: a C++ API and toolkit for analyzing and managing BAM files. *Bioinformatics* 27:1691–1692.

Bely M, Sablayrolles J-M, Barre P. 1990. Automatic detection of assimilable nitrogen deficiencies during alcoholic fermentation in oenological conditions. *J Ferment Bioeng.* 70:246–252.

Blateyron L, Sablayrolles JM. 2001. Stuck and slow fermentations in oenology: statistical study of causes and effectiveness of conbinated additions of oxygen and diammonium phosphate. *J Ferment Bioeng.* 91:184–189.

Bolger AM, Lohse M, Usadel B. 2014. Trimmomatic: a flexible trimmer for Illumina sequence data. *Bioinformatics* 30:2114–2120.

Borneman AR, Desany BA, Riches D, Affourtit JP, Forgan AH, Pretorius IS, Egholm M, Chambers PJ. 2011. Whole-genome comparison reveals novel genetic elements that characterize the genome of industrial strains of *Saccharomyces cerevisiae*. *PLoS Genet.* 7: e1001287.

Borneman AR, Forgan AH, Pretorius IS, Chambers PJ. 2008. Comparative genome analysis of a *Saccharomyces cerevisiae* wine strain. *FEMS Yeast Res.* 8:1185–1195.

Bourbouloux A. 2000. Hgt1p, a high affinity glutathione transporter from the yeast *Saccharomyces cerevisiae*. *J Biol Chem.* 275: 13259–13265.

Breslow DK, Cameron DM, Collins SR, Schuldiner M, Stewart-Ornstein J, Newman HW, Braun S, Madhani HD, Krogan NJ, Weissman JS. 2008. A comprehensive strategy enabling high-resolution functional analysis of the yeast genome. *Nat Methods.* 5:711–718.

Cai H, Hauser M, Naider F, Becker JM. 2007. Differential regulation and substrate preferences in two peptide transporters of *Saccharomyces cerevisiae*. *Eukaryot Cell.* 6:1805–1813.

Cheeseman K, Ropars J, Renault P, Dupont J, Gouzy J, Branca A, Abraham A, Ceppi M, Conseiller E, Debuchy R, et al. 2014. Multiple recent horizontal transfers of a large genomic region in cheese making fungi. *Nat Commun.* 5:2876.

Cheynier V, Souquet JM, Moutounet M. 1989. Glutathione content and glutathione to hydroxycinnamic acid ratio in *Vitis vinifera* grapes and musts. *Am J Enol Vitic.* 40:320–324.

Coelho MA, Gonçalves C, Sampaio JP, Gonçalves P. 2013. Extensive intra-kingdom horizontal gene transfer converging on a fungal fructose transporter gene. *PLoS Genet.* 9:e1003587.

Cromie GA, Hyma KE, Ludlow CL, Garmendia-Torres C, Gilbert TL, May P, Huang AA, Dudley AM, Fay JC. 2013. Genomic sequence diversity and population structure of *Saccharomyces cerevisiae* assessed by RAD-seq. *G3 (Bethesda)* 3:2163–2171.

Damon C, Vallon L, Zimmermann S, Haider MZ, Galeote V, Dequin S, Luis P, Fraissinet-Tachet L, Marmeisse R. 2011. A novel fungal family of oligopeptide transporters identified by functional metatranscriptomics of soil eukaryotes. *ISME J.* 9:67.

Deak T. 2007. Handbook of food spoilage yeasts. Boca Raton (FL): CRC Press.

Dunlop PC, Meyer GM, Ban D, Roon RJ. 1978. Characterization of two forms of asparaginase in *Saccharomyces cerevisiae*. *J Biol Chem.* 253: 1297–1304.

Fay JC, Benavides JA. 2005. Evidence for domesticated and wild populations of *Saccharomyces cerevisiae*. *PLoS Genet.* 1:66–71.

Fitzpatrick DA. 2011. Horizontal gene transfer in fungi. *FEMS Microbiol Lett.* 23:1574–6968.

Galeote V, Bigey F, Beyne E, Novo M, Legras JL, Casaregola S, Dequin S. 2011. Amplification of a *Zygosaccharomyces bailii* DNA segment in wine yeast genomes by extrachromosomal circular DNA formation. *PLoS One* 6:e17872.

Galeote V, Novo M, Salema-Oom M, Brion C, Valerio E, Goncalves P, Dequin S. 2010. *FSY1*, an horizontally transferred gene in the *Saccharomyces cerevisiae* EC1118 wine yeast strain encodes a high affinity fructose/H^+ symporter. *Microbiology* 156:3754–3761.

Gibson BR, Lawrence SJ, Boulton CA, Box WG, Graham NS, Linforth RS, Smart KA. 2008. The oxidative stress response of a lager brewing yeast strain during industrial propagation and fermentation. *FEMS Yeast Res.* 8:574–585.

Gladieux P, Ropars J, Badouin H, Branca A, Aguileta G, De Vienne DM, Rodriguez de la Vega RC, Branco S, Giraud T. 2014. Fungal evolutionary genomics provides insight into the mechanisms of adaptive divergence in eukaryotes. *Mol Ecol.* 23:753–773.

Gojkovic Z, Knecht W, Zameitat E, Warneboldt J, Coutelis JB, Pynyaha Y, Neuveglise C, Moller K, Loffler M, Piskur J. 2004. Horizontal gene transfer promoted evolution of the ability to propagate under anaerobic conditions in yeasts. *Mol Genet Genomics.* 271:387–393.

Grant CM, Perrone G, Dawes IW. 1998. Glutathione and catalase provide overlapping defenses for protection against hydrogen peroxide in the yeast *Saccharomyces cerevisiae*. *Biochem Biophys Res Commun.* 253:893–898.

Güldener U, Heck S, Fielder T, Beinhauer J, Hegemann JH. 1996. A new efficient gene disruption cassette for repeated use in budding yeast. *Nucleic Acids Res.* 24:2519–2524.

Hall C, Brachat S, Dietrich FS. 2005. Contribution of horizontal gene transfer to the evolution of *Saccharomyces cerevisiae*. *Eukaryot Cell.* 4:1102–1115.

Homann OR, Cai H, Becker JM, Lindquist SL. 2005. Harnessing natural diversity to probe metabolic pathways. *PLoS Genet.* 1:e80.

Ito K, Hikida A, Kawai S, Lan VT, Motoyama T, Kitagawa S, Yoshikawa Y, Kato R, Kawarasaki Y. 2013. Analysing the substrate multispecificity of a proton-coupled oligopeptide transporter using a dipeptide library. *Nat Commun.* 4:2502.

Jones DT, Taylor WR, Thornton JM. 1992. The rapid generation of mutation data matrices from protein sequences. *Comput Appl Biosci.* 8: 275–282.

Keeling PJ, Palmer JD. 2008. Horizontal gene transfer in eukaryotic evolution. *Nat Rev Genet.* 9:605–618.

Koonin EV, Wolf YI. 2008. Genomics of bacteria and archaea: the emerging dynamic view of the prokaryotic world. *Nucleic Acids Res.* 36: 6688–6719.

Kritzinger EC, Bauer FF, du Toit WJ. 2013. Role of glutathione in winemaking: a review. *J Agric Food Chem.* 61:269–277.

Kurtzman CP. 2003. Phylogenetic circumscription of *Saccharomyces*, *Kluyveromyces* and other members of the Saccharomycetaceae, and the proposal of the new genera *Lachancea*, *Nakaseomyces*, *Naumovia*, *Vanderwaltozyma* and *Zygotorulaspora*. *FEMS Yeast Res.* 4:233–245.

Kurtzman CP. 2011. Phylogeny of the ascomycetous yeasts and the renaming of *Pichia anomala* to *Wickerhamomyces anomalus*. *Antonie Van Leeuwenhoek* 99:13–23.

Landolfo S, Politi H, Angelozzi D, Mannazzu I. 2008. ROS accumulation and oxidative damage to cell structures in *Saccharomyces*. *Biochim Biophys Acta.* 1780:892–898.
League GP, Slot JC, Rokas A. 2012. The *ASP3* locus in *Saccharomyces cerevisiae* originated by horizontal gene transfer from *Wickerhamomyces*. *FEMS Yeast Res.* 12:859–863.
Lee JC, Straffon MJ, Jang TY, Higgins VJ, Grant CM, Dawes IW. 2001. The essential and ancillary role of glutathione in *Saccharomyces cerevisiae* analysed using a grande *gsh1* disruptant strain. *FEMS Yeast Res.* 1:57–65.
Lee YJ, Kim KJ, Kang HY, Kim HR, Maeng PJ. 2012. Involvement of *GDH3*-encoded $NADP^+$-dependent glutamate dehydrogenase in yeast cell resistance to stress-induced apoptosis in stationary phase cells. *J Biol Chem.* 287:44221–44233.
Legras JL, Merdinoglu D, Cornuet JM, Karst F. 2007. Bread, beer and wine: *Saccharomyces cerevisiae* diversity reflects human history. *Mol Ecol.* 16:2091–2102.
Li H, Durbin R. 2010. Fast and accurate long-read alignment with Burrows-Wheeler transform. *Bioinformatics* 26:589–595.
Liti G, Carter DM, Moses AM, Warringer J, Parts L, James SA, Davey RP, Roberts IN, Burt A, Koufopanou V, et al. 2009. Population genomics of domestic and wild yeasts. *Nature* 458:337–341.
Luo R, Liu B, Xie Y, Li Z, Huang W, Yuan J, He G, Chen Y, Pan Q, Liu Y, et al. 2012. SOAPdenovo2: an empirically improved memory-efficient short-read de novo assembler. *GigaScience* 1:18.
Madeo F, Fröhlich E, Ligr M, Grey M, Sigrist SJ, Wolf DH, Fröhlich KU. 1999. Oxygen stress: a regulator of apoptosis in yeast. *J Cell Biol.* 145:757–767.
Marcet-Houben M, Gabaldon T. 2009. The tree versus the forest: the fungal tree of life and the topological diversity within the yeast phylome. *PLoS One* 4:e4357.
Marinoni G, Manuel M, Petersen RF, Hvidtfeldt J, Sulo P, Piskur J. 1999. Horizontal transfer of genetic material among *Saccharomyces* yeasts. *J Bacteriol.* 181:6488–6496.
McDonald TR, Dietrich FS, Lutzoni F. 2012. Multiple horizontal gene transfers of ammonium transporters/ammonia permeases from prokaryotes to eukaryotes: toward a new functional and evolutionary classification. *Mol Biol Evol.* 29:51–60.
McGovern PE, Zhang J, Tang J, Zhang Z, Hall GR, Moreau RA, Nunez A, Butrym ED, Richards MP, Wang CS, et al. 2004. Fermented beverages of pre- and proto-historic China Life with 6000 genes. *Proc Natl Acad Sci U S A.* 101:17593–17598.
Mendes-Ferreira A, Sampaio-Marques B, Barbosa C, Rodrigues F, Costa V, Mendes-Faia A, Ludovico P, Leao C. 2010. Accumulation of non-superoxide anion reactive oxygen species mediates nitrogen-limited alcoholic fermentation by *Saccharomyces cerevisiae*. *Appl Environ Microbiol.* 76:7918–7924.
Nestelbacher R, Laun P, Vondrakova D, Pichova A, Schuller C, Breitenbach M. 2000. The influence of oxygen toxicity on yeast mother cell-specific aging. *Exp Gerontol.* 35:63–70.
Novo M, Bigey F, Beyne E, Galeote V, Gavory F, Mallet S, Cambon B, Legras JL, Wincker P, Casaregola S, et al. 2009. Eukaryote-to-eukaryote gene transfer events revealed by the genome sequence of the wine yeast *Saccharomyces cerevisiae* EC1118. *Proc Natl Acad Sci U S A.* 106:16333–16338.
Richards TA. 2011. Genome evolution: horizontal movements in the fungi. *Curr Biol.* 21:028.
Richards TA, Talbot NJ. 2013. Horizontal gene transfer in osmotrophs: playing with public goods. *Nat Rev Microbiol.* 11:720–727.
Ros VI, Hurst GD. 2009. Lateral gene transfer between prokaryotes and multicellular eukaryotes: ongoing and significant? *BMC Biol.* 7:20.
Sablayrolles JM, Barre P, Grenier P. 1987. Design of a laboratory automatic system for studying alcoholic fermentation in anisothermal enological conditions. *Biotechnol Tech.* 1:181–184.
Schacherer J, Shapiro JA, Ruderfer DM, Kruglyak L. 2009. Comprehensive polymorphism survey elucidates population structure of *Saccharomyces cerevisiae*. *Nature* 458:342–345.
Scheiner D. 1976. Determination of ammonia and kjeldahl nitrogen by endophenol method. *Water Res.* 10:31–36.
Schiestl RH, Gietz RD. 1989. High efficiency transformation of intact yeast cells using single stranded nucleic acids as a carrier. *Curr Genet.* 16:339–346.
Schonknecht G, Weber AP, Lercher MJ. 2014. Horizontal gene acquisitions by eukaryotes as drivers of adaptive evolution. *BioEssays* 36:9–20.
Slot JC, Hibbett DS. 2007. Horizontal transfer of a nitrate assimilation gene cluster and ecological transitions in fungi: a phylogenetic study. *PLoS One* 2:e1097.
Steels H, James SA, IRoberts N, Stratford M. 1999. *Zygosaccharomyces lentus* a significant new osmophilic, preservative-resistant spoilage yeast, capable of growth at low temperature. *J Appl Microbiol.* 87:520–527.
Tamura K, Peterson D, Peterson N, Stecher G, Nei M, Kumar S. 2011. MEGA5: molecular evolutionary genetics analysis using maximum likelihood, evolutionary distance, and maximum parsimony methods. *Mol Biol Evol.* 28:2731–2739.
Varela C, Pizarro F, Agosin E. 2004. Biomass content governs fermentation rate in nitrogen-deficient wine musts. *Appl Environ Microbiol.* 70:3392–3400.
Wang Y, Shirogane T, Liu D, Harper J. 2003. Exit from exit: resetting the cell cycle through Amn1 inhibition of G protein signalling. *Cell* 112:697–709.
Yokotsuka K, Fukui M. 2002. Changes in nitrogen compounds in berries of six grape cultivars during ripening over two years. *Am J Enol Vitic.* 53:69–77.
Yvert G, Brem RB, Whittle J, Akey JM, Foss E, Smith EN, Mackelprang R, Kruglyak L. 2003. Trans-acting regulatory variation in *Saccharomyces cerevisiae* and the role of transcription factors. *Nat Genet.* 35:57–64.